



1    **Title: Wildfire-induced disruptions to evapotranspiration, runoff, and water-balance  
2    closure across California's water supply watersheds**

3

4    **Authors:**

5    **Ziying Han<sup>1</sup>, Han Guo<sup>12\*</sup>, Michael L. Goulden<sup>3</sup>, Roger C. Bales<sup>12</sup>**

6

7    **Affiliations:**

8    <sup>1</sup> Department of Civil and Environmental Engineering, University of California, Berkeley, CA,  
9    USA

10    <sup>2</sup> Sierra Nevada Research Institute, University of California, Merced, CA, USA

11    <sup>3</sup> Department of Earth System Science, University of California, Irvine, Irvine, CA, USA

12    *\*Correspondence:* Han Guo (hguo7@berkeley.edu)

13

14

15

16



17 **Abstract**

18 Wildfire activity has intensified across forested mountain watersheds globally, yet the basin-scale  
19 hydrologic consequences of large, high-severity fires remain poorly quantified. Here we integrate  
20 four decades of satellite-derived evapotranspiration (ET), precipitation (P), full natural flow  
21 (FNF) records, and spatially explicit fire-perimeter data to evaluate how wildfire alters ET, basin  
22 outflow, and water-balance closure across major water-supply basins in California. High-severity  
23 fires consistently suppressed ET by 100–250 mm in the first postfire year, with recovery strongly  
24 modulated by vegetation traits, moisture availability, and disturbance recurrence. Structurally  
25 diverse and moisture-rich basins recovered 75% of prefire ET within 4–5 years, whereas drier,  
26 conifer-dominated systems required up to a decade. Although interannual P remained the  
27 dominant control on basin outflow, reduced ET partially offset drought-year declines in FNF  
28 within heavily burned sub-basins, indicating a localized compensatory effect. Water-balance  
29 analysis revealed systematic negative residuals ( $P - ET - FNF$ ) during years with substantial fire  
30 disturbance, demonstrating measurable departures from steady-state closure. Basin-specific  
31 diagnostics showed that these deviations arise from both disturbance-driven hydrologic shifts  
32 and observational uncertainties, including precipitation underestimation and stream-gauge bias.  
33 Proportional and two-parameter adjustments improved closure across most basins, underscoring  
34 the need for disturbance-aware calibration in regional water-balance assessments. Collectively,  
35 our findings reveal that wildfires act as short-term hydrologic shocks that suppress ET, alter  
36 basin outflow patterns, and distort modeled water budgets across fire-prone headwater systems.  
37 Incorporating fire history, disturbance intensity, and ET-recovery patterns into hydrologic models  
38 and reservoir operations will be essential for improving postfire flow prediction and sustaining  
39 long-term water-supply reliability in an increasingly disturbance-affected climate.

40 **Keywords:** wildfire, evapotranspiration, runoff, forest disturbance, water balance.



41 **1. Introduction**

42 Wildfire activity across the western United States has intensified dramatically over recent  
43 decades, driven by rising temperatures, prolonged droughts, and shifts in vegetation composition  
44 associated with climate change and historical land-use practices (Abatzoglou & Williams 2016;  
45 Williams et al. 2019; Westerling 2016). In California, this trend is especially pronounced: fire  
46 seasons have lengthened, large high-severity events have become more frequent, and cumulative  
47 burned area has expanded across montane-forest ecosystems historically shaped by infrequent,  
48 low-intensity fires (Keeley & Syphard 2016; Miller & Safford 2012; Westerling et al. 2006).  
49 These compound disturbances not only restructure forest composition but also exert cascading  
50 effects on watershed hydrology, with implications for water-supply reliability, flood control, and  
51 downstream ecosystem services (Paul et al., 2022, Robinne et al., 2021).

52 The hydrologic consequences of wildfire are mediated by changes in vegetation cover, soil  
53 properties, and energy exchange. Canopy loss reduces interception and transpiration, while soil  
54 combustion and hydrophobicity may alter infiltration and subsurface flow pathways (Hallema et  
55 al., 2017). These changes affect evapotranspiration (ET), a dominant component of the terrestrial  
56 water budget, and modify the partitioning of precipitation (P) into basin outflow, recharge, and  
57 storage. In the short term, postfire ET typically declines due to vegetation mortality surplus,  
58 potentially enhancing surface and shallow-subsurface runoff. Over time, as vegetation recovers,  
59 ET may gradually return toward prefire levels. However, the rate and completeness of recovery  
60 depend on fire severity, postfire climate, and landscape context (Boisramé et al. 2017; Roche et  
61 al. 2020).

62 These shifts in hydrologic partitioning have significant implications for water supply in  
63 California, a state where water availability and demand are geographically misaligned. The  
64 majority of P falls in the northern mountains, while water use in the southern and central regions  
65 exceeds supply. To bridge this divide, California has constructed extensive redistribution  
66 infrastructure, including the Central Valley Project and the State Water Project (California  
67 Department of Water Resources, 2023). These systems rely heavily on consistent basin outflow  
68 from snow-fed mountain basins, many of which are now increasingly affected by high-severity  
69 wildfire. As fire disturbs vegetation cover, soil structure, and water fluxes in these source  
70 watersheds, the reliability of downstream supply may be undermined. Ensuring long-term water  
71 security in California will therefore depend not only on engineered conveyance systems but also  
72 on active management and protection of upstream hydrologic sources, particularly in fire-prone  
73 landscapes (Wayburn 2019).

74 ET is not only a dominant flux in the water balance but also a diagnostic indicator of ecosystem  
75 disturbance and recovery. It reflects both biological attributes (e.g., leaf area, rooting depth) and  
76 physical drivers (e.g., temperature, radiation), and responds dynamically to shifts in land cover



77 and climate (Roche et al. 2020). In managed mountain watersheds that support regional water  
78 supply, fluctuations in ET can serve as a sensitive indicator of ecosystem disturbance and  
79 hydrologic change, particularly following wildfire (Chung et al., 2024). Because ET integrates  
80 vegetation structure, physiological activity, and energy availability, fire-induced shifts in canopy  
81 cover or soil properties may propagate through the broader water cycle. Deviations between  
82 expected (P–ET) and basin outflow (FNF) therefore provide a window into how wildfire  
83 modifies vegetation water use, soil-water interactions, and basin-scale routing, highlighting the  
84 need to understand these processes to assess postfire hydrologic behavior (Guzmán-Rojo et al.,  
85 2024).

86 While many studies have explored fire–hydrology interactions using paired catchments,  
87 empirical regressions, or process-based models (Atwood et al., 2023, Bart & Tague, 2017, Bart,  
88 2016), there remains a critical gap in basin-to-regional scale analyses that directly integrate  
89 disturbance history, satellite-derived ET, and observed basin outflow across water-supplying  
90 watersheds. The absence of such data-integrated assessments limits our ability to empirically  
91 trace how wildfire-driven vegetation loss and regrowth translate into hydrologic consequences,  
92 resulting in insufficient guidance for water managers to anticipate postfire changes in water  
93 availability and diagnose hydrologic anomalies in heavily disturbed source watersheds.

94 In this study, we address these knowledge gaps by analyzing wildfires, evapotranspiration, and  
95 observed basin outflow patterns over the last four decades across five major northern California  
96 watersheds that serve as critical water sources for the state. We combine fire-perimeter data from  
97 the California Fire and Resource Assessment Program (FRAP), gridded hydrologic data from the  
98 Center for Ecosystem Climate Solutions (CECS), and long-term FNF records from the California  
99 Data Exchange Center (CDEC). This integrated dataset enables us to evaluate: (1) how ET  
100 responds to and recovers from wildfires across watersheds with varying climate and terrain; (2)  
101 in what ways wildfires influence annual basin outflow in major water-supply basins; and (3) how  
102 wildfires and other factors contribute to water-balance-closure errors across basins, and how  
103 these imbalances can be diagnosed.

## 104 2. Methods

105 To assess how wildfires reshape ET, runoff, and basin-scale water balance across California’s  
106 critical water-supply watersheds, we conducted an integrated fire–hydrology analysis that links  
107 disturbance history, remote-sensing-derived ET, and observed full natural flow (FNF) through  
108 annual mass-balance relationships. This approach directly operationalizes the three research  
109 questions outlined above by tracing postfire ET changes, evaluating wildfire influences on basin  
110 outflow (FNF), and examining the stability of the water-balance relation (P – ET versus FNF)  
111 under varying disturbance conditions.

### 112 2.1 Study areas



113 The Trinity, Upper Sacramento, McCloud, Pit, and Feather watersheds (Table 1, Figure 1) span  
114 the Cascade Range and the northern Sierra Nevada, with elevations from 200 meters to over  
115 4300 meters (Mount Shasta). These watersheds drain into both Shasta Lake and Oroville  
116 Reservoir, and to the Sacramento River, and exhibit diverse topographic and climatic  
117 characteristics.

118 The Trinity, McCloud, and Upper Sacramento River watersheds lie in Northern California's  
119 Klamath-Cascade region and share steep mountainous terrain, deep incised canyons, and  
120 pronounced elevation gradients that support dense mixed-conifer forests, primarily composed of  
121 Douglas-fir, ponderosa pine, white fir, and sugar pine. These areas receive substantial winter  
122 precipitation, with high-elevation snow accumulation driving spring runoff. Mount Shasta  
123 strongly influences the McCloud and Upper Sacramento, contributing snowmelt and volcanic  
124 springs to cold, perennial flows. The Pit watershed features volcanic soils and groundwater-fed  
125 baseflow, but receives less precipitation overall and has a drier climate as it descends into lower  
126 agricultural valleys. In contrast, the Feather watershed in the Sierra Nevada covers forested  
127 western ridges and drier eastern slopes that occupy the Sierra Nevada rain shadow. Its hydrology  
128 is regulated by both volcanic terrain and infrastructure such as Oroville Dam, which manages  
129 downstream water deliveries and flood control.

130 These watersheds experience a Mediterranean climate, characterized by wet, cold winters and  
131 long, dry summers. Precipitation occurs primarily between November and March, with  
132 significant snowfall at higher elevations. Annual precipitation varies from around 400 mm in the  
133 lower elevations of the Pit watershed to over 3000 mm at higher elevations in the Upper  
134 Sacramento watershed. Winter temperatures range from -5°C to 9°C, while summer temperatures  
135 range from 10°C to 25°C, depending on elevation (PRISM Climate Group).

## 136 **2.2 Data**

137 To analyze fire impacts, we used the historical fire-perimeter dataset from the Fire and Resource  
138 Assessment Program (FRAP) (<https://www.fire.ca.gov/what-we-do/fire-resource-assessment-program>), focusing on 37 fires exceeding 10,000 acres between 1985 and 2020 (Table 2).  
139 Given the overlapping fire boundaries and shared ecological characteristics, we combined the  
140 Trinity, Upper Sacramento, and McCloud watersheds into a unified area (MTUS) to analyze fire  
141 impacts at a broader scale while maintaining hydrologic relevance. The Center for Ecosystem  
142 Climate Solutions (CECS) (<https://california-ecosystem-climate.solutions>) provides annual  
143 evapotranspiration (ET) and precipitation (P) raster products from 1985 to 2024 at 30-m  
144 resolution, derived from its internal water-balance calculations. These datasets have been widely  
145 used in previous studies (Guo et al., 2023; Chung et al., 2024).

146 Additionally, we obtained monthly full natural flow (FNF) data from the California Data  
147 Exchange Center (CDEC) (<https://cdec.water.ca.gov/index.html>). This dataset includes nine



149 continuously monitored sites within key water-supply watersheds, spanning from 1985 to the  
150 2023 water year (Table 3). Using California's digital elevation model (DEM) and the Watershed  
151 tool in ArcGIS Pro, we delineated the contributing area for each FNF site to ensure consistent  
152 spatial matching among P, ET, and FNF.

153 **2.3 Analysis**

154 **Quantifying ET reduction and recovery.** We assessed the net ET response to wildfire by  
155 comparing burned and unburned areas before and after each fire. Areas within each watershed  
156 that have never experienced fire and that fall within a 500-m buffer surrounding each fire  
157 perimeter were defined as unburned areas. The net ET reduction in burned area was calculated as  
158 follows (Roche et al., 2020):

159 
$$\Delta ET = (ET_{burned, postfire} - ET_{unburned, postfire}) - (ET_{burned, prefire} - ET_{unburned, prefire}) \quad (1)$$

160 where  $ET_{burned, prefire}$  and  $ET_{unburned, prefire}$  represent the mean ET in the five years preceding a fire,  
161 and  $ET_{burned, postfire}$ ,  $ET_{unburned, postfire}$  denote ET after the fire. When fewer than five pre-fire years  
162 were available, ET was averaged from 1985 until the year of the fire. This paired approach  
163 isolates the net disturbance signal by removing background climatic variability. For each  
164 watershed, we calculated the cumulative burned area and averaged  $\Delta ET$  over burned pixels to  
165 derive both per-area reduction (mm) and total volumetric change ( $km^3$ ). ET recovery was tracked  
166 annually following each fire, and the time required for ET to reach 75% of the five-year pre-fire  
167 mean was used as the recovery benchmark.

168 **Assessing wildfire impacts on runoff response.** To evaluate how wildfires influence runoff  
169 generation in key water-supply watersheds, we examined the relationships among P, ET, and  
170 observed basin outflow (FNF) at the sub-basin scale. For each water year from 1985 to 2023, we  
171 used FRAP fire-perimeter data to calculate the annual proportion of burned area within each  
172 delineated sub-watershed. Corresponding annual P and ET values were obtained from CECS  
173 gridded datasets and area-averaged for each sub-watershed. Monthly FNF records from CDEC  
174 were aggregated to annual totals and matched to their upstream contributing areas. We then  
175 compared interannual variation in P, ET, and FNF for each sub-basin, focusing on whether  
176 reductions in ET, particularly in fire years, were associated with observable changes in FNF. We  
177 also evaluated potential lagged effects of wildfire by examining FNF anomalies one to three  
178 years after major fire events.

179 **Diagnosing wildfire-induced disruption to basin-scale water balance.** To evaluate whether  
180 wildfire influences water-balance closure, we compared annual residuals ( $P - ET - FNF$ )  
181 between high-fire years and non-fire years. High-fire years were defined as those in which more  
182 than 3% of the watershed area burned, a threshold chosen to identify years with substantial  
183 disturbance; all remaining years were classified as non-fire years. A Welch's two-sample t-test



184 was used to assess whether this difference reflects a systematic effect of wildfire on hydrologic  
185 closure.

186 To further assess basin-scale water balance, we compared annual  $P - ET$  with observed FNF for  
187 each sub-watershed. Under steady-state conditions ( $\Delta S \approx 0$ ),  $P - ET$  should closely match FNF.  
188 Deviations from the 1:1 relationship were therefore used to identify potential imbalance and  
189 diagnose hydrologic processes such as enhanced deep infiltration, preferential subsurface  
190 routing, or unaccounted surface flows. For each site, we examined linear relationships among  
191 FNF,  $P$ , and  $P - ET$ . Where persistent discrepancies existed, we applied proportional adjustments  
192 to either  $P$  or FNF, depending on which correction produced improved alignment, to interpret  
193 which component contributed most to the imbalance. Watersheds were grouped into categories  
194 such as: basins exhibiting minimal imbalance; basins requiring scaling of  $P$  or FNF; and basins  
195 requiring both scaling and an intercept correction. These adjustments were used solely as  
196 diagnostic tools rather than for calibration or data fitting.

197 **3. Results**

198 **3.1 Quantifying ET reduction and recovery**

199 Wildfires caused substantial reductions in ET across burned areas, ranging from 40 to 440 mm  
200  $yr^{-1}$  depending on fire severity and vegetation conditions, with the strongest suppression  
201 occurring in the first postfire year (Table 2; Figures 2). ET gradually increased in subsequent  
202 years as vegetation recovered.

203 Following the 1987 Lost Fire in the Pit basin, ET in the 92  $km^2$  burned area declined by 177 mm  
204 in the first postfire year (16 million  $m^3$ ) and accumulated to 83 million  $m^3$  over the eight years  
205 required for ET to return to 75% of its prefire mean. The 1992 Fountain Fire, also in the Pit and  
206 characterized by high severity and a large burned extent (244  $km^2$ ), produced a first-year ET  
207 reduction of 439 mm (107 million  $m^3$ ) and a cumulative reduction of 960 million  $m^3$  before  
208 reaching the 75% recovery threshold in year 12. In 1993, the combined effects of multiple fires  
209 resulted in a net ET reduction of 347 mm across burned areas in the Pit basin (Figure S1). In the  
210 Feather basin, the 2007 Moonlight Fire burned 263  $km^2$  and generated a first-year ET reduction  
211 of 325 mm (85 million  $m^3$ ). ET recovered to 75% of its prefire value by year 8, yielding a  
212 cumulative loss of 452 million  $m^3$  (Figure S2). The 2008 Motion Fire in MTUS caused a first-  
213 year reduction of 292 mm across 115  $km^2$ , corresponding to 33 million  $m^3$ , and a cumulative  
214 impact of 79 million  $m^3$  over the three-year recovery period (Figure S3). These examples show  
215 that both burn severity and burned area govern the magnitude and duration of ET reductions.  
216 Cumulative losses ranged from tens to hundreds of millions of cubic meters before partial  
217 recovery was achieved.



218 Net ET reductions at the watershed scale were derived using area-weighted averages across all  
219 fires within each basin. In the Pit basin, repeated fires between 1993 and 2011 produced  
220 substantial interannual variability in net ET reduction, yet total reductions remained relatively  
221 stable until 2005, declining steadily thereafter (Figure 2c). The 2012 fires burned 617 km<sup>2</sup>,  
222 producing a larger total ET reduction (147 million m<sup>3</sup>) despite a modest per-area reduction (75  
223 mm, Figure 2a-b). In the Feather basin, fluctuations in net ET reduction reflected both fire  
224 severity and the re-burning of previously affected areas. From 1988 to 2017, reductions ranged  
225 between 75 and 163 mm yr<sup>-1</sup>, generally lower than in the Pit (Figure 2b). However, successive  
226 large fires between 2018 and 2020 sharply increased both burned area and basin-wide ET  
227 reduction. Although MTUS experienced fewer fires overall, its events were relatively severe.  
228 Three overlapping fires in 2018 burned 421 km<sup>2</sup> and led to a per-area ET reduction of 143 mm,  
229 equivalent to 420 million m<sup>3</sup> of total reduction. Among the three basins, the Feather experienced  
230 the largest individual fires (Table 2), whereas the Pit experienced the slowest rate of ET  
231 recovery.

232 Across the 37 fires examined, post-fire ET recovery occurred steadily with time, but repeated  
233 fires often prevented full return to prefire conditions. Because ET reductions were concentrated  
234 in the first postfire year, due to the use of annual ET, the second postfire year was considered the  
235 first year of recovery. On average, ET recovered 18% in this first recovery year, with some fires  
236 (e.g., Loyalton) reaching 67%. Most fires (31 of 37) reached 75% recovery within an average of  
237 3.9 years (range: 1–12 years). Fires that had not reached 75% recovery by 2023 were excluded  
238 from this calculation.

239 At the watershed scale (Figure 3), the Pit basin showed the slowest recovery, requiring an  
240 average of 10 years to reach 75% of prefire ET, followed by MTUS (5 years) and Feather (4  
241 years). Five years after a fire, ET had recovered to 69% of prefire levels in the Pit, 75% in  
242 MTUS, and 78% in the Feather (Table 2). In the Feather basin, recovery was interrupted by large  
243 fires occurring in years 9 and 21, lowering ET sharply (by ~100 mm), but subsequent recovery  
244 rates were faster than after the initial fire. Similar patterns of partial recovery followed by  
245 renewed suppression were observed in MTUS, where secondary fires occurred 11 years after  
246 initial burning.

### 247 **3.2 Assessing wildfire impacts on basin outflow**

248 At the sub-basin scale, evapotranspiration is influenced by both wildfire and dry years, while  
249 annual basin outflow, represented by observed full natural flow, is primarily driven by  
250 precipitation and shows a small but detectable response to changes in ET (Figure 4). For  
251 example, although no fires occurred in the DAV region between 1985 and 2020, ET still  
252 exhibited fluctuations, indicating that regional climate variability played a substantial role  
253 (Figure 4a). Between 1985 and 2023, two major declines in ET occurred in DAV. The first



254 decline, from 1987 to 1992, involved a 17% reduction in ET and coincided with sharp ET  
255 decreases in other basins, driven by low precipitation and corresponding reductions in basin  
256 outflow. The second notable decline occurred in 2022, when ET decreased by 20% relative to the  
257 preceding five-year average during another dry year.

258 This 2022 decline was synchronized across nearly all sub-watersheds in the Feather basin,  
259 particularly in areas overlapping with the 2020 North Complex and 2021 Dixie fires, where ET  
260 dropped sharply, by 58% and 54%, respectively, following extensive high-severity canopy loss  
261 (Figure S4). The strong spatial coherence likely reflects the combined impacts of drought and the  
262 two large fires, which together produced a broad, contiguous burn footprint and reduced  
263 vegetation water use across the region. However, the modest increase in P in 2022 introduces  
264 uncertainty in interpreting the observed increase in basin outflow. The FTO station, which  
265 represents basin-wide outflow for the Feather, captured these variations (Figure 4b). Although  
266 the Feather experienced frequent fires, the limited proportion of burned area prior to 2021  
267 constrained fire impacts on whole-basin ET. The rapid ET declines observed in 2021 and 2022  
268 were therefore likely dominated by the 2021 fire.

269 Across all basins, interannual P variation was strongly correlated with annual FNF, indicating  
270 that precipitation remains the dominant control on basin outflow. Because most fires affected  
271 only small fractions of sub-basin areas, ET reductions were generally insufficient to produce  
272 measurable changes in FNF at gauging stations. A notable exception occurred in the ANT basin  
273 in 2007, where a fire burned 47% of the basin area and reduced ET by 31% (Figure 4c). In the  
274 same year, P declined by 26%, yet FNF decreased by only 10%, suggesting that reduced ET  
275 partially offset the precipitation deficit. However, quantifying this compensatory effect requires  
276 information on subsurface storage changes, which were not available.

### 277 **3.3 Diagnosing wildfire-induced disruption and water-balance closure across basins**

278 To assess whether wildfire contributes to basin-scale water-balance discrepancies, we compared  
279 annual residuals of P – ET and full natural flow (P – ET – FNF) between high-fire years and  
280 non-fire years across all basins from 1985 to 2023. High-fire years were defined as years in  
281 which more than 3% of the watershed area burned (n = 13), while all remaining years were  
282 classified as non-fire years (n = 54). High-fire years consistently exhibited more negative  
283 residuals, indicating that observed FNF exceeded expected P – ET to a greater degree during  
284 periods of extensive fire activity (Figure S5). A Welch's two-sample t-test confirmed that the  
285 difference was statistically significant ( $t = -2.76$ ,  $p = 0.017$ ), demonstrating that years with  
286 extensive fire activity systematically depart from hydrologic closure relative to non-fire years.

287 To further evaluate the nature of these discrepancies, we analyzed the relationships between FNF,  
288 P, and P – ET using annual data from nine study watersheds. Under ideal conditions, modeled P  
289 and ET should closely reproduce observed runoff, resulting in well-aligned P – ET and FNF



290 curves. In basins where ET remains stable and unaffected by disturbance, a near-linear  
291 relationship between P and FNF is expected, with data points clustering along the 1:1 line  
292 (reflecting annual storage change) and a slope approaching unity. However, substantial  
293 deviations from this ideal behavior were observed, reflecting combined influences of data  
294 uncertainties, basin heterogeneity, and disturbance legacies (Roche et al., 2022).

295 To diagnose the sources of imbalance, we applied basin-specific adjustments to P or FNF.  
296 Watersheds were grouped into three categories based on closure behavior. First, for well-  
297 balanced basins with good alignment between P-ET and FNF, such as those in the upper Feather  
298 watershed (Figure 5a,b), FNF vs. P and P – ET vs. P exhibited consistent relationships, and only  
299 minor proportional adjustment (e.g., 1.01 scaling of FNF in FRD) was needed for  
300  $P - ET - FNF \approx 0$ . Second, in basins where  $FNF > P - ET$  (e.g., DAV), the imbalance likely arose  
301 from underestimated precipitation. Multiplying P by 1.03 reduced residuals to near zero, aligning  
302 with previous evidence of precipitation underestimation in mountainous terrain. Third, in other  
303 basins,  $P - ET > FNF$ , suggesting incomplete runoff measurement. Applying a proportional  
304 scaling to FNF reduced these discrepancies; for example, in FTO, a small adjustment achieved a  
305 post-correction residual of 132 mm (Figure 5c).

306 For several basins (e.g., PSH, MSS, SIS), large residuals persisted even after proportional  
307 adjustment. The intersection of regression lines indicated structural bias rather than simple  
308 scaling errors. Introducing a second parameter (intercept) to adjust FNF produced near-perfect  
309 alignment between P – ET and FNF, reducing residuals to within 50 mm and confirming that  
310 multi-parameter corrections better captured hydrologic consistency (Figure 5d,e; Figure S6).

311 Overall, this basin-level diagnosis demonstrates that deviations from closure stem from a  
312 combination of disturbance-induced hydrologic shifts, input-data biases, and structural  
313 measurement errors. Identifying and classifying these imbalances enables clearer interpretation  
314 of hydrologic responses to wildfire and improves the reliability of regional water-balance  
315 assessments.

316 **4. Discussion**

317 Understanding how wildfires alter ET, basin outflow (FNF), and overall water balance is  
318 essential for diagnosing watershed resilience and supporting adaptive water-resource  
319 management in fire-prone landscapes. This study contributes new insights into (1) the magnitude  
320 and variability of ET reduction and recovery following wildfire of different extent and severity,  
321 (2) the extent to which fire-induced ET suppression influences observed outflow, and (3) the  
322 spatial heterogeneity and diagnostic interpretation of water-balance closure across multiple  
323 watersheds. Our multi-basin, post-fire hydrologic assessment highlights the need to reconcile  
324 spatial patterns, disturbance history, and observational uncertainty to better characterize  
325 watershed-scale impacts.



326 **4.1 Determinants of postfire ET suppression and recovery patterns**

327 Postfire reductions in ET were largely controlled by burn severity and burned area, producing  
328 first-year unit-area losses of 100 to 250 mm per year, consistent with canopy combustion, loss of  
329 transpiring leaf area, and reductions in soil water retention (Mappin et al. 2003; Clemente et al.  
330 2005; Nolan et al. 2014; Roche et al. 2018; Baur et al. 2024). High-severity events such as the  
331 1992 fires in the Pit watershed (242 mm ET loss over 244 km<sup>2</sup>) and the 2018 fires in the MTUS  
332 (143 mm over 421 km<sup>2</sup>) illustrate this strong suppression, and align with previous findings that  
333 high-severity burns in the Sierra Nevada produce early ET losses around 265 mm, with  
334 moderate-severity burns reducing ET by 150 to 200 mm over multiple years and requiring more  
335 than 15 years for full recovery in severely affected areas (Roche et al. 2020; Ma et al. 2020).

336 Recovery trajectories varied across basins and reflected vegetation structure, climatic water  
337 availability, and disturbance history. Feather and MTUS showed faster recovery, returning to 75  
338 percent of prefire ET within four to five years, supported by favorable moisture conditions and  
339 rapid regrowth of fire-adapted shrubs. Pit, with a drier climate and repeated high-severity fires,  
340 recovered more slowly, reaching only 69 percent of prefire ET by year five and requiring  
341 approximately ten years to meet the 75 percent threshold. These patterns are consistent with  
342 hydrologic stress associated with drought and persistent soil-moisture deficits (Silveiro et al.  
343 2024). Across the 37 fires, 31 reached 75 percent recovery within an average of 3.9 years,  
344 although several remained below this threshold by 2023, underscoring the importance of species  
345 traits. Shrub communities frequently resprouted quickly, but long-term ET recovery depended on  
346 tree canopy regeneration, and surviving conifers may experience long-term physiological  
347 impairment that limits transpiration (Niccoli et al. 2023).

348 Vegetation composition patterns derived from CECS datasets further highlight the central role of  
349 postfire structural change in governing ET recovery (Figures S1–S3). In high-severity burns such  
350 as the 2007 Bucks fire (Figure S3c), ET declined sharply and remained suppressed as shrubs and  
351 herbaceous cover increased relative to trees. A similar trajectory occurred in the Scotch fire  
352 footprint (Figure S3j), where the 2008 burn was followed by reburning during the 2020–2021  
353 North Complex event, illustrating how repeated disturbance can constrain canopy re-  
354 establishment and prolong low-ET states. Even modest increases in low-stature vegetation  
355 combined with delayed tree regrowth contributed to sustained watershed-scale ET suppression  
356 extending more than a decade in some areas.

357 Climatic and ecological heterogeneity across basins further shaped cumulative responses.  
358 MTUS, despite having the smallest burned area, experienced the highest total ET loss during the  
359 2018 fire (420 million m<sup>3</sup>), while Feather, which accumulated the largest burned area from 1985  
360 to 2022, exhibited pronounced increases in total ET loss after successive fires between 2018 and  
361 2022. These patterns emphasize that repeated disturbance is a major constraint on hydrologic



362 recovery and that forests with complex canopy structure, functional diversity, and high  
363 ecological elasticity tend to recover more rapidly. In contrast, it has been suggested that  
364 ecosystems such as the Russian River watershed showed limited ET response, likely due to deep  
365 soils, Mediterranean climate, and buffering from subsurface storage and fire-adapted vegetation  
366 (Newcomer et al. 2023). Postfire soil hydrophobicity may also suppress ET by reducing  
367 infiltration and enhancing overland flow, a mechanism more relevant in coarse-textured or  
368 shallow volcanic soils such as in the Pit basin (Huffman et al. 2001; Boisramé et al. 2019).

369 Taken together, our results show that the magnitude of initial ET loss is controlled by burn  
370 severity and burned area, the pace of recovery is governed by vegetation regrowth pathways and  
371 moisture availability, and long-term suppression arises from disturbance recurrence. These  
372 factors jointly explain the heterogeneous ET responses observed across California's water-supply  
373 basins and provide the ecological basis for interpreting subsequent impacts on basin outflow and  
374 water-balance closure.

#### 375 **4.2 Drivers of postfire runoff response**

376 Although interannual precipitation variability remains the dominant driver of runoff patterns  
377 across most basins, our results suggest that postfire reductions in ET may partially offset  
378 precipitation declines, particularly in high-severity burn areas. In most cases, runoff closely  
379 tracked precipitation trends, while ET fluctuated more moderately. However, the ANT basin  
380 illustrates a potential compensatory mechanism. After a 2007 fire reduced ET by 31%, reduction  
381 in ET, runoff declined by only 10% despite 26% lower annual precipitation. This divergence  
382 suggests that suppressed ET may enhance water availability for basin outflow (FNF) under  
383 certain conditions. Mechanistically, fire-induced canopy loss and root mortality reduce  
384 transpiration and interception (Ice et al. 2004; Ma et al. 2020), while soil water repellency can  
385 inhibit infiltration and promote surface runoff (Shakesby & Doerr 2006; Pradhan & Floyd 2021).  
386 Together, these processes shift hydrologic partitioning toward runoff, particularly in water-  
387 limited systems where vegetation loss is extensive (Boisramé et al. 2019; Bart et al. 2021;  
388 Guzmán-Rojo et al. 2024).

389 However, such effects were not consistently detectable across all basins due to scale and context.  
390 Most fires affected limited portions of each watershed, limiting their measurable hydrologic  
391 impact at larger scale. Consistent with other studies, significant runoff responses typically  
392 emerge only when  $\geq 20$ –30% of a watershed is burned (Wine & Cadol 2016; Newcomer et al.  
393 2023). Additionally, topographic complexity, vegetation recovery rates, and subsurface storage  
394 can modulate responses, making it difficult to isolate ET impacts (Kinoshita & Hogue 2011;  
395 Wilder & Kinoshita 2022). For example, in the Feather basin, postfire ET dropped sharply in  
396 2022, but concurrent increases in precipitation obscured runoff attribution. Limited spatial  
397 coverage of stream gauges and ET monitoring hampers inference, especially at sub-basin



398 scales. While remote sensing has improved ET estimation (Poon & Kinoshita 2018; Lahmers et  
399 al. 2025), establishing causal links between ET reduction and runoff response remains difficult  
400 without high-resolution hydrometeorological networks. These challenges underscore the  
401 importance of spatial scale, burn extent, and observational capacity in understanding postfire  
402 hydrologic responses.

403 **4.3 Diagnosing and correcting postfire water-balance closure errors**

404 Wildfire disturbance emerged as an important driver of deviations from expected water-balance  
405 closure across California's major watersheds. As shown in our analysis, fire years consistently  
406 exhibited more negative residuals ( $P - ET - FNF$ ), indicating that observed basin outflow (FNF)  
407 systematically exceeded modeled  $P - ET$  during and immediately after disturbance. This  
408 divergence demonstrates that wildfires can create short-term hydrologic imbalances, enhancing  
409 basin outflow or subsurface losses beyond what steady-state  $P - ET$  frameworks predict. Likely  
410 mechanisms include reduced canopy interception, increased overland and subsurface flow,  
411 accelerated snowmelt, and postfire changes in infiltration capacity. These findings are consistent  
412 with earlier plot- and catchment-scale observations showing that fire simplifies canopy structure  
413 and redistributes water fluxes, often producing a transient "hydrologic release" followed by  
414 delayed recovery (Kinoshita & Hogue, 2015, Williams et al., 2022).

415 However, disturbance alone cannot explain the full range of discrepancies among basins. Even  
416 under non-disturbed conditions, achieving water-balance closure across California's  
417 heterogeneous landscapes requires careful interpretation and basin-specific adjustment strategies.  
418 Climatic gradients, lithologic differences, and variable human regulation contribute to strong  
419 spatial heterogeneity in the relationship between simulated ( $P - ET$ ) and observed (FNF) fluxes.  
420 Our diagnostic framework categorized nine sub-basins into three closure types, each reflecting  
421 distinct physical and measurement characteristics.

422 In contrast, the DAV watershed exhibited FNF consistently exceeding  $P - ET$ , which is unlikely  
423 due to enhanced runoff generation given consistent ET simulation methods across basins.  
424 Instead, this discrepancy likely reflects precipitation underestimation. A modest 3% increase in  
425 the gridded precipitation substantially reduced residuals, aligning with prior findings that sparse  
426 station density and complex terrain in California's mountains often lead to interpolation errors  
427 (Avanzi et al. 2020; Safeeq et al. 2021, Roche et al. 2022). Orographic and localized rainfall  
428 patterns, common in such regions, may further exacerbate this issue (Avanzi et al. 2020). The  
429 DAV case underscores that seemingly excessive FNF may reflect incomplete precipitation  
430 inputs, emphasizing the need for finer-resolution meteorological data and improved validation.

431 In other basins (e.g., FTO, ANT, TNL, SDT),  $P - ET$  exceeded FNF, suggesting that FNF  
432 observations may underestimate actual water yield. This systematic underestimation likely  
433 results from subsurface bypass flow, vertical seepage, or unmeasured groundwater discharge



434 (Avanzi et al. 2020; Roche et al. 2022). Permeable lithology, faulting, and reservoir operations  
435 further obscure true basin outflow (Safeeq et al. 2021; Roche et al. 2022). Applying proportional  
436 corrections reduced residuals to within 100–150 mm, indicating that flow underestimation was  
437 the dominant error in these cases.

438 However, in PSH, MSS, and SIS, large residuals persisted even after proportional adjustment,  
439 and regression lines exhibited crossing patterns, signaling structural bias beyond simple scaling  
440 errors. Potential causes include gauge misalignment, cross-sectional changes, or sensor drift  
441 (Safeeq et al. 2021; Roche et al. 2022). Here, we applied a dual-parameter correction (scaling +  
442 intercept), which improved alignment and reduced residuals to within 50 mm. This suggests that  
443 in basins with mixed error sources, flexible calibration models that reflect physical measurement  
444 processes are necessary for reliable water balance closure.

445 Achieving water-balance closure across heterogeneous basins requires context-specific  
446 correction strategies, as no single method universally resolves discrepancies. Proportional  
447 adjustments are suitable for diagnosing fluxes where systematic underestimation dominates and  
448 temporal patterns are coherent, while dual-parameter approaches are more appropriate in basins  
449 with structural biases or complex error signatures. Critically, identifying the underlying sources  
450 of imbalance, rather than enforcing statistical fit, enhances the physical credibility of hydrologic  
451 assessments under multi-source uncertainty. Nonetheless, even error-informed corrections face  
452 practical limitations. P and ET inputs often rely on spatial interpolation or remotely sensed  
453 products, which may fail to capture localized variability in regions with complex terrain or  
454 sparse monitoring infrastructure. Similarly, full natural flow (FNF) estimates can be  
455 compromised by stream-gauge placement and design, particularly when gauges do not align with  
456 actual contributing areas, resulting in long-term structural bias. In addition, many watersheds  
457 may be affected by data gaps or inaccurately reported upstream diversions, reservoir operations,  
458 and inter-basin transfers, complicating attribution of observed runoff deficits. These constraints  
459 reduce the generalizability of empirical corrections and highlight the need for next-generation  
460 hydrologic models that couple high-resolution observations, detailed management records, and  
461 process-based representations of watershed behavior.

#### 462 **4.4 Implications for hydrologic modeling and water resource management**

463 Wildfires disrupt the balance among precipitation, ET, and basin outflow in ways that  
464 conventional hydrologic models do not fully capture. The systematic deviations between  
465 modeled (P–ET) and observed basin outflow (FNF) during fire years show that disturbance  
466 fundamentally alters basin water budgets. Postfire ET suppression, delayed vegetation recovery,  
467 and shifts in infiltration or snowmelt processes create hydrologic conditions that steady-state  
468 models cannot represent. These findings highlight the need for disturbance-sensitive model



469 components, including flexible ET recovery functions, representations of vegetation structural  
470 change, and nonlinear thresholds linking burn extent to runoff response.

471 At the basin-integration scale, wildfire effects interact with substantial observational  
472 uncertainties. Persistent negative P–ET–FNF residuals reflect not only process-level shifts but  
473 also precipitation underestimation, gauge bias, and heterogeneous subsurface pathways. No  
474 single correction approach ensures water-balance closure across diverse terrain; instead, models  
475 should pair physically based process representations with diagnostic calibration schemes that  
476 explicitly account for disturbance and measurement uncertainty. Such strategies will reduce  
477 misinterpretation of postfire hydrologic anomalies and improve runoff estimation in complex  
478 landscapes.

479 From a management perspective, incorporating fire history, burn severity, and ET recovery  
480 patterns into reservoir operations and water-allocation planning is essential for avoiding  
481 overestimation of water availability or underestimation of infrastructure vulnerability. Ultimately,  
482 reliable water-balance assessments in fire-prone regions will require integrating high-resolution  
483 disturbance mapping, continuous ET and precipitation monitoring, and process-based  
484 ecohydrologic modeling to anticipate watershed responses to wildfire, drought, and climate  
485 variability and support resilient water-resource governance.

#### 486 **5. Conclusions**

487 Large wildfires impose short-term but measurable disruptions to evapotranspiration, basin  
488 outflow, and water-balance closure in California’s major water-supply watersheds. High-severity  
489 burns suppressed ET by 100–250 mm in the first year, with recovery rates governed by  
490 vegetation traits, moisture availability, and disturbance recurrence. Although precipitation  
491 remained the primary control on basin outflow, ET losses occasionally moderated drought-year  
492 flow declines in heavily burned basins, indicating a limited compensatory effect. Fire years also  
493 produced systematically negative P–ET–FNF residuals, revealing that wildfire amplifies existing  
494 closure errors from precipitation underestimation and stream-gauge bias. Together, these results  
495 show that wildfire acts as a hydrologic shock that alters water partitioning and exposes structural  
496 uncertainties in observational datasets. Incorporating disturbance history, ET-recovery patterns,  
497 and closure diagnostics will improve postfire flow prediction and strengthen water-resource  
498 planning under rising fire activity.



499 **Table 1. Information for California key water supply watersheds**

Watershed	Area, km <sup>2</sup>	Elevation range, m	Topography	Hydrologic influence	Precipitation range/mean, mm
Trinity	1861	573 - 2751	Mountainous terrain	Snowmelt and precipitation contribute to river systems	756 - 2626 / 1399
Upper Sacramento	1551	178 - 4069	Mountainous terrain	Snowmelt and volcanic springs from Mount Shasta contribute to cold, clear rivers	810 - 3003 / 1572
McCloud	1773	306 - 4306	Mountainous terrain	Snowmelt and volcanic springs contribute to river systems	772 - 2526 / 1413
Pit	14,753	301 - 3161	Gradual terrain at lower elevations with alluvial valleys; volcanic soils	Groundwater from volcanic aquifers and snowmelt influence river flows	432 - 1081 / 665
Feather	9335	221 - 2773	Diverse terrain: high altitude in west and center, decreasing south and north	Influenced by volcanic activity and regulated by Oroville Dam, impacting water distribution and flood control	547 - 1982 / 1085

500

501



502 **Table 2. Information for 37 large fires in key water supply watersheds**

Fire Name	Year	Area burned, km <sup>2</sup>	5-year pre-fire ET average, mm	ET change <sup>1</sup>		Years to recovery <sup>3</sup>	Map ID
				First-year post-fire, mm <sup>2</sup>	Cumulative ET reduction over recovery period, million m <sup>3</sup>		
<b><i>Pit</i></b>							
Lost	1987	92	370	-178	83	8	29
Fountain	1992	244	701	-439	960	12	18
Damon/Long	1996	95	239	-84	8	1	28
Jones	2000	106	682	-256	27	1	19
Blue	2001	139	381	-157	81	5	17
Bear	2004	42	626	-330	31	3	30
Corral Fire	2008	50	336	-136	38	7	31
Bagley	2012	186	880	-279	80	3	20
Barry Point	2012	376	379	-224	210	3	21
Reading	2012	114	480	-239	259*	/	24
Bald	2014	161	334	-139	37	2	22
Eiler	2014	130	497	-322	254*	/	23
Day	2014	53	470	-298	116*	/	32
Cove	2017	125	359	-163	68	5	25
Stone	2018	160	306	-95	26	2	26
W-5 Cold Springs	2020	344	191	-39	5	2	16
Gold	2020	92	319	-132	30*	/	27
<b><i>Feather</i></b>							
Clark (Plumas #531)	1987	162	687	-141	124	8	5
Cottonwood	1994	195	296	-233	138	4	4
Bucks	1999	139	644	-196	47	2	6
Storrie	2000	227	750	-224	205	5	7
Wheeler	2007	90	656	-229	58	4	12
Moonlight	2007	263	352	-325	452	8	3
South-Frey	2008	50	818	-169	8	1	14
Scotch	2008	53	785	-173	9	1	15
Cub	2008	60	833	-98	38	6	13
Btu Lightning Complex	2008	217	597	-290	209	4	8
Chips	2012	309	653	-239	330	4	9
Camp	2019	621	472	-297	532	4	10
Walker	2020	221	461	-232	140	4	11
Loyalton	2020	189	240	-82	17	2	1
Sheep	2020	120	496	-251	68*	/	2
<b><i>MTUS</i></b>							
Sheep #1	1999	50	774	-209	19	2	37
Motion	2008	115	717	-292	79	3	33
Carr	2018	930	715	-277	917*	/	34
Delta	2018	257	752	-393	398*	/	35
Hirz	2018	164	815	-240	71	2	36



503 **Table 2. Information for 37 large fires in key water supply watersheds (Cont.)**

504 <sup>1</sup> ET data is based on net ET reduction.

505 <sup>2</sup>Minus indicates a reduction relative to the previous year

506 <sup>3</sup>Years to recovery was defined as the number of years after the fire until the mean annual ET equaled or exceeded 75% of the  
507 pre-fire 5-year mean. /: ET recovery did not reach 75% in the available years of data.

508 \*The mean annual ET did not reach 75% of the pre-fire 5-year mean in the available years of data.

509

510

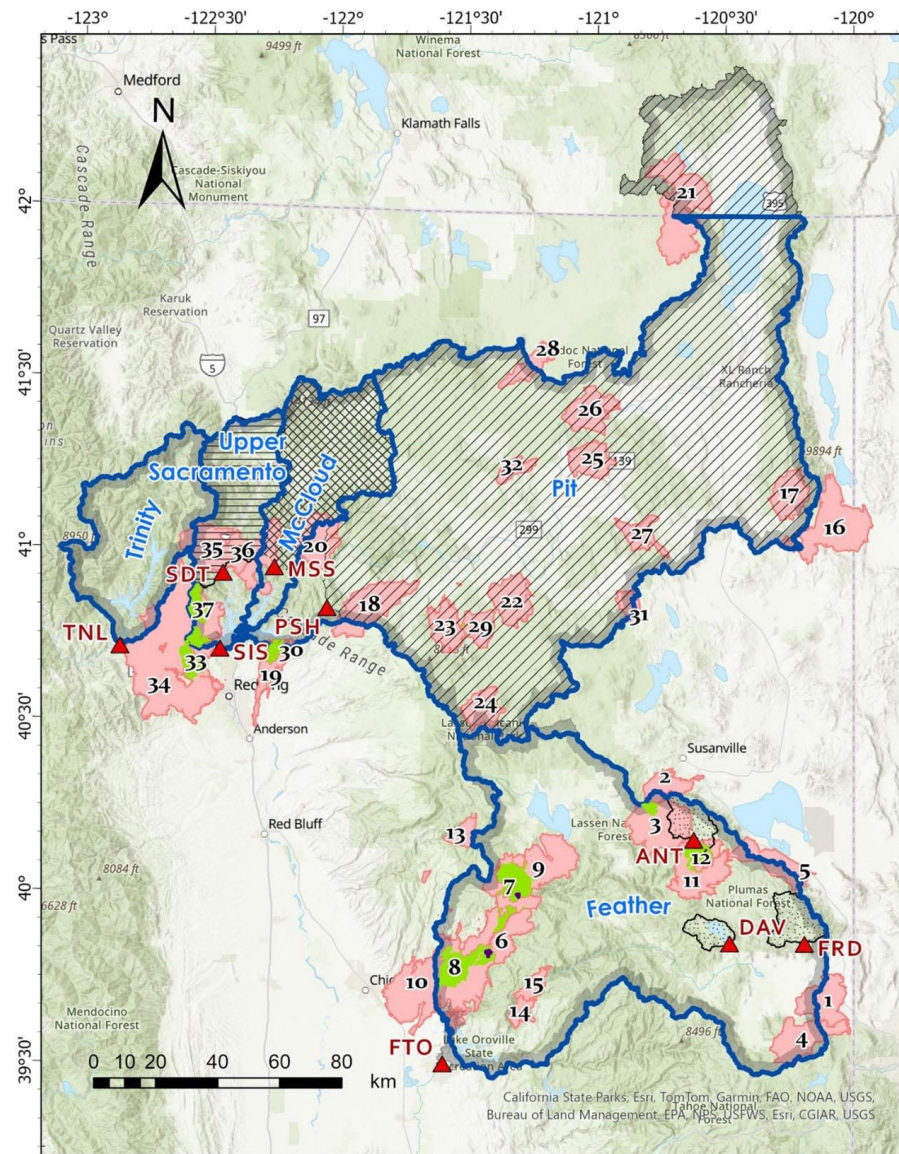


511 **Table 3. Information for CDEC FNF stations in key water supply watersheds**

Station Name	Station ID	Area, km <sup>2</sup>	Average annual value, mm				WBal <sup>1</sup>
			P	ET	FNF	P-ET	
Lake Davis (DWR)	DAV	115	707	410	322	296	1.03P
Frenchman Dam	FRD	214	478	350	131	128	1.01FNF
Antelope Lake	ANT	184	634	443	207	191	1.05FNF
Feather River at							
Oroville	FTO	9482	1084	522	538	562	1.08FNF
Sacramento R at							
Delta	SDT	1102	1525	644	895	881	1.01FNF
McCloud R abv L							
Shasta	MSS	1569	1391	630	871	760	1.74FNF-0.75
Trinity R at							
Lewiston	TNL	1863	1399	575	820	824	1.03FNF
Pit River at Shasta							
Lake	PSH	16176	613	347	209	265	2.44FNF-0.25
Sacto Inflow-Shasta	SIS	19995	787	408	329	379	1.67FNF-0.17

512 <sup>1</sup>Water-balance components were adjusted, with the number preceding 'P' or 'FNF' indicating the  
513 multiplier applied to the data.

514

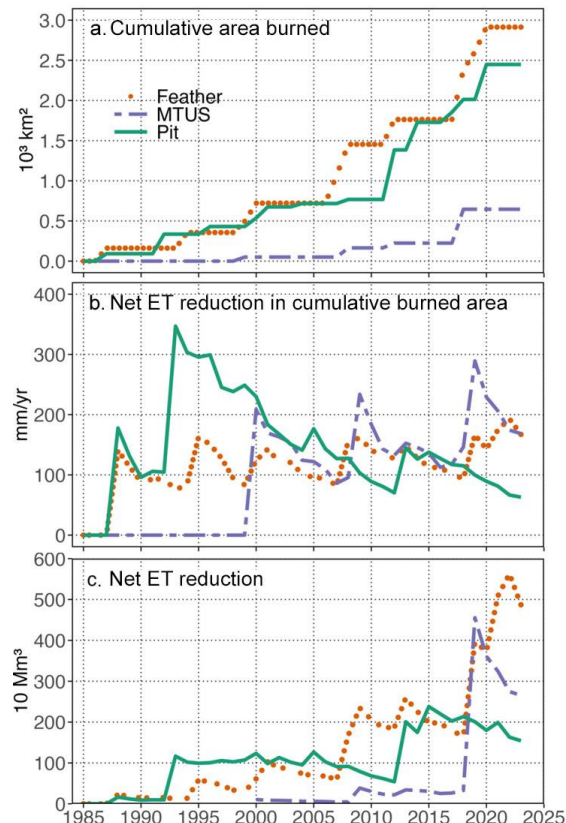


515

516 **Figure 1.**

517 Study area. The blue outlined watersheds are the five key water supply watersheds. Red triangles are  
518 sites with full natural flow (FNF) data, and shaded areas are the corresponding watersheds. The pink  
519 parts are areas showing the 37 large fires analyzed. The green and dark purple parts respectively indicate  
520 areas that burned twice and three times. Table 1 and Table 2 list the information on FNF sites and large  
521 fires.

522



523

524 **Figure 2.**

525 Net evapotranspiration (ET) reductions and cumulative area burned in the three study areas. (a)  
526 cumulative area burned (Table 2), (b) Net annual ET reduction depth per unit area burned (See Figure S  
527 1 to 3 for ET declines due to individual fire and increases with regrowth), and (c) net annual ET  
528 reduction volume resulting from fires in the three watersheds 1985–2023 (product of data on panels a  
529 and b).

530

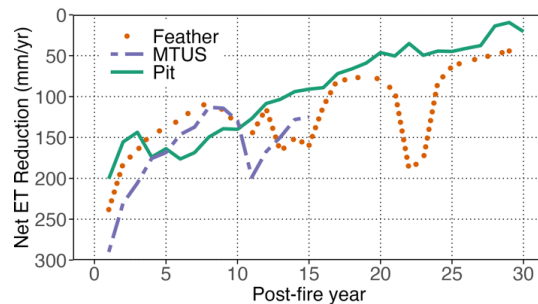


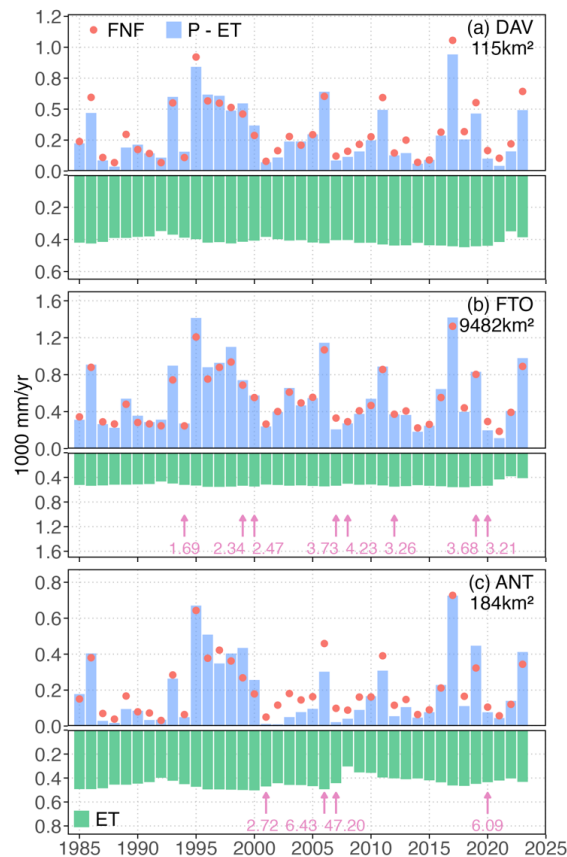
531

532 **Figure 3.**

533 Post-fire ET recovery. Post-fire evapotranspiration (ET) recovery trajectories were tracked over 30 years  
534 across three watersheds: Feather (orange dots), MTUS (purple dashed line), and Pit (green solid line).  
535 The y-axis shows net ET reduction (mm/year) relative to pre-fire conditions. Data reflect averaged  
536 changes across burned areas, with at least three fire events. While all three watersheds exhibit gradual  
537 ET recovery, the rate and magnitude vary, and Feather displays notable variability in later post-fire  
538 years.

539

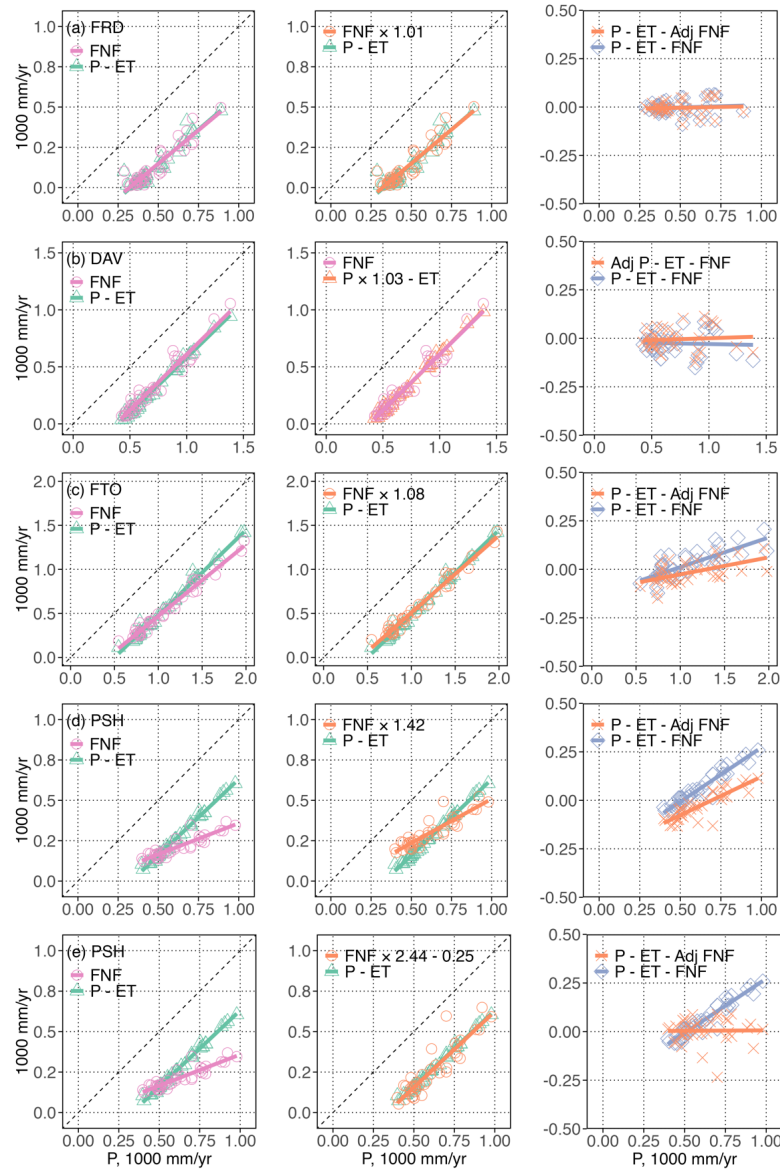




540 **Figure 4.**

541 Changes in precipitation, evapotranspiration, full natural flow, and burned area from 1985 to 2023 in the  
542 Feather basin. The changes in ET, P, P-ET and FNF over time for the sub-watersheds are located. The  
543 pink arrows and labels indicate the year of fire and the percentage of burned area. The figures only show  
544 years where the area burned was greater than 1% of the area of the watershed. Data for additional sites  
545 are in Supplementary Figure S6.

546  
547  
548  
549



550 **Figure 5.**

551 Water balance analysis of representative watersheds. Show unadjusted annual water balance constituent  
 552 discharge (FNF) and precipitation minus evapotranspiration (P-ET) versus annual precipitation (P).  
 553 Also, adjust the FNF or P values (with one or two parameters) to improve the agreement between P-ET  
 554 and FNF. The dashed diagonal line is a 1:1 line. Water balance residuals (P-ET-FNF) using unadjusted  
 555 and adjusted components. Data for additional sites is in Supplementary Figure S7 and S8.

556



557 **Data availability**

558 The wildfire perimeter dataset is publicly available through the California Fire and Resource Assessment  
559 Program (FRAP). Full natural flow (FNF) records are publicly available from the California Data  
560 Exchange Center (CDEC). The evapotranspiration and precipitation datasets generated by the Center for  
561 Ecosystem Climate Solutions (CECS) were previously publicly accessible; access is currently provided  
562 upon request from CECS.  
563 Derived watershed-scale metrics and analysis scripts are available from the corresponding author upon  
564 reasonable request.

565 **Author contributions**

566 Conceptualization: ZH, RB. Data curation: ZH, MG, HG. Formal analysis: ZH, HG. Methodology: ZH,  
567 HG, RB. Project administration: RB. Resources: RB, MG. Software: ZH, HG. Supervision: RB.  
568 Validation: ZH. Visualization: ZH. Writing – original draft: ZH. Writing – review and editing: all  
569 authors.

570 **Competing interests**

571 The authors declare that they have no conflict of interest.

572 **Acknowledgements**

573 We thank the Center for Ecosystem Climate Solutions (CECS) for providing the datasets used in this  
574 study, which was supported by the California Climate Investments program through the Strategic  
575 Growth Council (grant no. CCR20021).



576 **References:**

577 Abatzoglou, J. T., & Williams, A. P. (2016). Impact of anthropogenic climate change on wildfire across western  
578 US forests. *Proceedings of the National Academy of Sciences of the United States of America*, 113(42),  
579 11770–11775. <https://doi.org/10.1073/pnas.1607171113>

580 Atwood, A., Hille, M., Clark, M. K., Rengers, F., Ntarlagiannis, D., Townsend, K., & West, A. J. (2023).  
581 Importance of subsurface water for hydrological response during storms in a post-wildfire bedrock  
582 landscape. *Nature Communications*, 14(1). <https://doi.org/10.1038/s41467-023-39095-z>

583 Avanzi, F., Rungee, J., Maurer, T., Bales, R., Ma, Q., Glaser, S., & Conklin, M. (2020). Climate elasticity of  
584 evapotranspiration shifts the water balance of Mediterranean climates during multi-year droughts. *Hydrology*  
585 and *Earth System Sciences*. <https://doi.org/10.5194/hess-24-4317-2020>

586 Bart, R. R. (2016). A regional estimate of postfire streamflow change in California. *Water Resources Research*,  
587 52(2), 1465–1478. <https://doi.org/10.1002/2014WR016553>

588 Bart, R. R., Ray, R. L., Conklin, M. H., Safeeq, M., Saksa, P. C., Tague, C. L., & Bales, R. C. (2021). Assessing  
589 the effects of forest biomass reductions on forest health and streamflow. *Hydrological Processes*, February,  
590 1–17. <https://doi.org/10.1002/hyp.14114>

591 Bart, R. R., & Tague, C. L. (2017). The impact of wildfire on baseflow recession rates in California. *Hydrological*  
592 *Processes*, 31(8), 1662–1673. <https://doi.org/10.1002/hyp.11141>

593 Baur, M. J., Friend, A. D., & Pellegrini, A. F. A. (2024). Widespread and systematic effects of fire on plant–soil  
594 water relations. *Nature Geoscience*, 17(11), 1115–1120. <https://doi.org/10.1038/s41561-024-01563-6>

595 Boisramé, G. F. S., Thompson, S. E., Tague, C. (Naomi), & Stephens, S. L. (2019). Restoring a Natural Fire  
596 Regime Alters the Water Balance of a Sierra Nevada Catchment. *Water Resources Research*, 55(7), 5751–  
597 5769. <https://doi.org/10.1029/2018WR024098>

598 Boisramé, G., Thompson, S., Collins, B., & Stephens, S. (2017). Managed Wildfire Effects on Forest Resilience  
599 and Water in the Sierra Nevada. *Ecosystems*, 20(4), 717–732. <https://doi.org/10.1007/s10021-016-0048-1>

600 California Department of Water Resources. (2023). *California Water Plan Update 2023*.  
601 <https://water.ca.gov/Programs/California-Water-Plan/Update-2023>.

602 Chung, M. G., Guo, H., Nyelele, C., Egoh, B. N., Goulden, M. L., Keske, C. M., & Bales, R. C. (2024). Valuation  
603 of forest-management and wildfire disturbance on water and carbon fluxes in mountain headwaters.  
604 *Ecohydrology*, February. <https://doi.org/10.1002/eco.2642>

605 Clemente, A. S., Rego, F. C., & Correia, O. A. (2005). Growth, water relations and photosynthesis of seedlings  
606 and resprouts after fire. *Acta Oecologica*, 27(3), 233–243. <https://doi.org/10.1016/j.actao.2005.01.005>

607 Guo, H., Goulden, M., Chung, M. G., Nyelele, C., Egoh, B., Keske, C., Conklin, M., & Bales, R. (2023). Valuing  
608 the benefits of forest restoration on enhancing hydropower and water supply in California's Sierra Nevada.  
609 *Science of The Total Environment*, 876, 162836. <https://doi.org/10.1016/j.scitotenv.2023.162836>

610 Guzmán-Rojo, M., Fernandez, J., D'Abzac, P., & Huysmans, M. (2024). Impacts of Wildfires on Groundwater  
611 Recharge: A Comprehensive Analysis of Processes, Methodological Challenges, and Research  
612 Opportunities. In *Water (Switzerland)* (Vol. 16, Issue 18). <https://doi.org/10.3390/w16182562>

613 Hallema, D. W., Sun, G., Bladon, K. D., Norman, S. P., Caldwell, P. V., Liu, Y., & McNulty, S. G. (2017).  
614 Regional patterns of postwildfire streamflow response in the Western United States: The importance of  
615 scale-specific connectivity. *Hydrological Processes*, 31(14), 2582–2598. <https://doi.org/10.1002/hyp.11208>

616 Huffman, E. L., MacDonald, L. H., & Stednick, J. D. (2001). Strength and persistence of fire-induced soil



617 hydrophobicity under ponderosa and lodgepole pine, Colorado Front Range. *Hydrological Processes*,  
618 15(15), 2877–2892. <https://doi.org/10.1002/hyp.379>

619 Ice, G. G., Neary, D. G., & Adams, P. W. (2004). Effects of Wildfire on Processes. *Journal of Forestry*,  
620 102(September), 16–20.

621 Keeley, J. E., & Syphard, A. D. (2016). Climate change and future fire regimes: Examples from California.  
622 *Geosciences (Switzerland)*, 6(3), 1–14. <https://doi.org/10.3390/geosciences6030037>

623 Kinoshita, A. M., & Hogue, T. S. (2011). Spatial and temporal controls on post-fire hydrologic recovery in  
624 Southern California watersheds. *Catena*, 87(2), 240–252. <https://doi.org/10.1016/j.catena.2011.06.005>

625 Kinoshita, A. M., & Hogue, T. S. (2015). Increased dry season water yield in burned watersheds in Southern  
626 California. *Environmental Research Letters*, 10(1). <https://doi.org/10.1088/1748-9326/10/1/014003>

627 Lahmers, T. M., Kumar, S. V., Ahmad, S. K., Holmes, T., Getirana, A., Orland, E., Locke, K., Biswas, N. K., Nie,  
628 W., Pflug, J., Whitney, K., Anderson, M., & Yang, Y. (2025). An Observation-Driven Framework for  
629 Modeling Post-Fire Hydrologic Response: Evaluation for Two Central California Case Studies. *Water  
630 Resources Research*, 61(2). <https://doi.org/10.1029/2023WR036582>

631 Ma, Q., Bales, R. C., Rungee, J., Conklin, M. H., Collins, B. M., & Goulden, M. L. (2020). Wildfire controls on  
632 evapotranspiration in California's Sierra Nevada. *Journal of Hydrology*, 590.  
633 <https://doi.org/10.1016/j.jhydrol.2020.125364>

634 Mappin, K. A., Pate, J. S., & Bell, T. L. (2003). Productivity and water relations of burnt and long-unburnt semi-  
635 arid shrubland in Western Australia. *Plant and Soil*, 257(2), 321–340.  
636 <https://doi.org/10.1023/A:1027349501441>

637 Miller, J. D., & Safford, H. (2012). Trends in wildfire severity: 1984 to 2010 in the Sierra Nevada, Modoc  
638 Plateau, and southern Cascades, California, USA. *Fire Ecology*, 8(3), 41–57.  
639 <https://doi.org/10.4996/fireecology.0803041>

640 Newcomer, M. E., Underwood, J., Murphy, S. F., Ulrich, C., Schram, T., Maples, S. R., Peña, J., Siirila-  
641 Woodburn, E. R., Trotta, M., Jasperse, J., Seymour, D., & Hubbard, S. S. (2023). Prolonged Drought in a  
642 Northern California Coastal Region Suppresses Wildfire Impacts on Hydrology. *Water Resources Research*,  
643 59(8). <https://doi.org/10.1029/2022WR034206>

644 Niccolli, F., Pacheco-Solana, A., Delzon, S., Kabala, J. P., Asgharinia, S., Castaldi, S., Valentini, R., & Battipaglia,  
645 G. (2023). Effects of wildfire on growth, transpiration and hydraulic properties of *Pinus pinaster* Aiton  
646 forest. *Dendrochronologia*, 79(January), 126086. <https://doi.org/10.1016/j.dendro.2023.126086>

647 Nolan, R. H., Lane, P. N. J., Benyon, R. G., Bradstock, R. A., & Mitchell, P. J. (2014). Changes in  
648 evapotranspiration following wildfire in resprouting eucalypt forests. *Ecohydrology*, 7(5), 1363–1377.  
649 <https://doi.org/10.1002/eco.1463>

650 Paul, M. J., LeDuc, S. D., Lassiter, M. G., Moorhead, L. C., Noyes, P. D., & Leibowitz, S. G. (2022). Wildfire  
651 Induces Changes in Receiving Waters: A Review With Considerations for Water Quality Management. *Water  
652 Resources Research*, 58(9). <https://doi.org/10.1029/2021WR030699>

653 Poon, P. K., & Kinoshita, A. M. (2018). Estimating evapotranspiration in a post-fire environment using remote  
654 sensing and machine learning. *Remote Sensing*, 10(11). <https://doi.org/10.3390/rs10111728>

655 Pradhan, N. R., & Floyd, I. (2021). Event based post-fire hydrological modeling of the upper Arroyo Seco  
656 watershed in southern California. *Water (Switzerland)*, 13(16). <https://doi.org/10.3390/w13162303>

657 PRISM Climate Group, Oregon State University, <https://prism.oregonstate.edu>.



658 Robinne, F. N., Hallema, D. W., Bladon, K. D., Flannigan, M. D., Boisramé, G., Bréthaut, C. M., Doerr, S. H., Di  
659 Baldassarre, G., Gallagher, L. A., Hohner, A. K., Khan, S. J., Kinoshita, A. M., Mordecai, R., Nunes, J. P.,  
660 Nyman, P., Santín, C., Sheridan, G., Stoof, C. R., Thompson, M. P., ... Wei, Y. (2021). Scientists' warning  
661 on extreme wildfire risks to water supply. *Hydrological Processes*, 35(5), 1–11.  
662 https://doi.org/10.1002/hyp.14086

663 Roche, J. W., Goulden, M. L., & Bales, R. C. (2018). Estimating evapotranspiration change due to forest  
664 treatment and fire at the basin scale in the Sierra Nevada, California. *Ecohydrology*, 11(7), 1–10.  
665 https://doi.org/10.1002/eco.1978

666 Roche, J. W., Ma, Q., Rungee, J., & Bales, R. C. (2020). Evapotranspiration Mapping for Forest Management in  
667 California's Sierra Nevada. *Frontiers in Forests and Global Change*.  
668 https://doi.org/10.3389/ffgc.2020.00069

669 Roche, J. W., Wilson, K. N., Ma, Q., & Bales, R. C. (2022). Water balance for gaged watersheds in the Central  
670 Sierra Nevada, California and Nevada, United States. *Frontiers in Forests and Global Change*, 5(July), 1–  
671 16. https://doi.org/10.3389/ffgc.2022.861711

672 Safeeq, M., Bart, R. R., Pelak, N. F., Singh, C. K., Dralle, D. N., Hartsough, P., & Wagenbrenner, J. W. (2021).  
673 How realistic are water-balance closure assumptions? A demonstration from the southern sierra critical zone  
674 observatory and kings river experimental watersheds. *Hydrological Processes*, 35(5), 1–16.  
675 https://doi.org/10.1002/hyp.14199

676 Shakesby, R. A., & Doerr, S. H. (2006). Wildfire as a hydrological and geomorphological agent. *Earth-Science  
677 Reviews*, 74(3–4), 269–307. https://doi.org/10.1016/j.earscirev.2005.10.006

678 Silveiro, A. C., Silvério, D. V., Macedo, M. N., Coe, M. T., Maracahipes, L., Uribe, M., Maracahipes-Santos, L.,  
679 Oliveira, P. T. S., Rattis, L., & Brando, P. M. (2024). Droughts Amplify Soil Moisture Losses in Burned  
680 Forests of Southeastern Amazonia. *Journal of Geophysical Research: Biogeosciences*, 129(10), 1–15.  
681 https://doi.org/10.1029/2024JG008011

682 Westerling, A. L., Hidalgo, H. G., Cayan, D. R., & Swetnam, T. W. (2006). Warming and earlier spring increase  
683 Western U.S. forest wildfire activity. *Science*, 313(5789), 940–943. https://doi.org/10.1126/science.1128834

684 Westerling, A. L. R. (2016). Increasing western US forest wildfire activity: Sensitivity to changes in the timing of  
685 spring. *Philosophical Transactions of the Royal Society B: Biological Sciences*, 371(1696).  
686 https://doi.org/10.1098/rstb.2015.0178

687 Wilder, B. A., & Kinoshita, A. M. (2022). Incorporating ECOSTRESS evapotranspiration in a paired catchment  
688 water balance analysis after the 2018 Holy Fire in California. *Catena*, 215(March), 106300.  
689 https://doi.org/10.1016/j.catena.2022.106300

690 Williams, A. P., Abatzoglou, J. T., Gershunov, A., Guzman-Morales, J., Bishop, D. A., Balch, J. K., &  
691 Lettenmaier, D. P. (2019). Observed Impacts of Anthropogenic Climate Change on Wildfire in California.  
692 *Earth's Future*, 7(8), 892–910. https://doi.org/10.1029/2019EF001210

693 Williams, A. P., Livneh, B., McKinnon, K. A., Hansen, W. D., Mankin, J. S., Cook, B. I., Smerdon, J. E., Varuolo-  
694 Clarke, A. M., Bjarke, N. R., Juang, C. S., & Lettenmaier, D. P. (2022). Growing impact of wildfire on  
695 western US water supply. *Proceedings of the National Academy of Sciences of the United States of America*,  
696 119(10), 1–8. https://doi.org/10.1073/pnas.2114069119

697 Wine, M. L., & Cadol, D. (2016). Hydrologic effects of large southwestern USA wildfires significantly increase  
698 regional water supply: Fact or fiction? *Environmental Research Letters*, 11(8). https://doi.org/10.1088/1748-  
699 9326/11/8/085006